Studies on tetraborane(8) carbonyl, $B_4H_8 \cdot CO$: its isomeric composition in the gas phase and in solution, and its reactions with alkenes [1]

Simon J. Cranson, Mark A. Fox, Robert Greatrex *, Norman N. Greenwood [2]

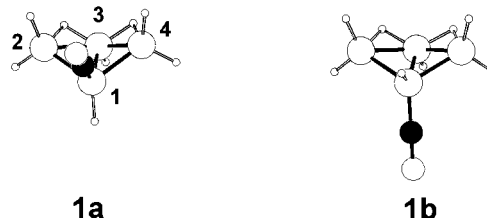*School of Chemistry, University of Leeds, Leeds, LS2 9JT, UK*

Abstract

^{11}B NMR spectra of tetraborane(8) carbonyl, $B_4H_8 \cdot CO$ **1**, reveal a changeover in the distribution of isomers in going from toluene solution to the gas phase. Fortuitously the distribution is 60:40 in each case, but comparison with published electron diffraction data and ab initio/IGLO computations indicates that the CO group is disposed endo with respect to the B_4 'butterfly' framework in the predominant isomer in the gas phase, and exo in solution. The results also allow conclusions to be drawn about the geometries of other $B_4H_8 \cdot L$ isomers on the basis of their reported proton NMR chemical shifts. Reactions of $B_4H_8 \cdot CO$ with ethene and propene at ca. 30 bar yield products, $R_4B_4H_4 \cdot CO$ (R = Et **2** or Pr³ **3**), in which all four wingtip hydrogen atoms of the tetraborane carbonyl have been replaced by alkyl groups. Variable-temperature ^{11}B and ^{1}H NMR spectra of **2** and **3** reveal interesting fluxional behaviour. © 1998 Elsevier Science S.A.

Keywords: Tetraborane(8) carbonyl; Boranes; Organoboranes; Hydroboration; Fluxionality; Geometrical isomerism

1. Introduction

Tetraborane(8) carbonyl, $B_4H_8 \cdot CO$, has been shown to exist as two geometrical isomers in an approximately 60:40 ratio, both by NMR studies of the (n-pentane) solution [1], and by electron diffraction analysis of the gaseous mixture [2]. The latter investigation demonstrated that the endo isomer **1a** predominates in the gas phase, and it was thought at the time that this was also the case in solution. Later, high level ab initio geometry optimisations gave satisfactory agreement with the gas-phase structures and with the 60:40 ratio, and computed IGLO [11]B chemical shift values also gave good agreement with experiment [3,4]. However, it was noted that the values for the endo isomer fitted better with the experimental NMR data for the exo isomer **1b** and vice versa [3]. To resolve this problem we have undertaken a detailed NMR study of $B_4H_8 \cdot CO$ in the gas phase and in solution.

1a   **1b**

The reaction chemistry of $B_4H_8 \cdot CO$ was studied in the 1960s by Spielman and Burg, who showed that the molecule was attacked by basic reagents such as diethyl ether, water and triethylamine to form involatile products without liberation of CO [5]. Ethene was also found to 'fix' the CO in a compound of low volatility, for which the formula was determined to be $(C_2H_4)_4B_4H_8CO$. The details of the structure were not established, and it was not clear whether the ethene was entering the molecule as ethyl groups, or (at least partially) in the form of bridging $B-CH_2CH_2-B$ groups as, for example, in the 'basket' derivatives of B_4H_{10}

---

* Corresponding author. E-mail: R.Greatrex@chem.leeds.ac.uk.
[1] Dedicated to Professor Ken Wade on the occasion of his 65th birthday in recognition of his outstanding contributions to the chemistry of the boranes, organometallics, and Main Group chemistry generally.
[2] Also corresponding author.

[6,7]. We now report the results of a detailed NMR study which establishes unequivocally the structure, not only of this compound, but also of an analogous derivative formed in the $B_4H_8 \cdot CO$–propene reaction.

2. Results and discussion

2.1. ^{11}B NMR data for $B_4H_8 \cdot CO$

The gas-phase [11]B{[1]H} spectrum of $B_4H_8 \cdot CO$ at ambient temperature consisted of several broad peaks corresponding to $B_4H_8 \cdot CO$ and its known [8] decomposition products, B_5H_{11}, B_4H_{10}, B_5H_9 and B_2H_6. [3] The peaks expected for boron atoms B(2), B(3) and B(4) were not well resolved owing to interference from the B(2,5) resonance of B_5H_{11}. However, the region of the spectrum corresponding to boron atoms at the 1 position was free from interfering resonances, and was very informative. This is reproduced in Fig. 1(a), together with the corresponding region of the spectrum obtained on $B_4H_8 \cdot CO$ as a solution in toluene-d_8—Fig. 1(b). The gas-phase spectrum can be interpreted in terms of two overlapping peaks with areas in the approximate ratio 40:60, consistent with the results of the electron diffraction study. Taken together, these two studies enable the component of the spectrum at more negative chemical shift to be assigned to the more abundant endo isomer. This conclusion is also seen to be in agreement with the ab initio IGLO computations (Table 1), which predict that the endo isomer **1a** is energetically more stable than the exo isomer **1b**, and that its B(1) resonance should indeed have a more negative chemical shift than that of the exo isomer.

In toluene solution there is a reversal in the intensities of the two peaks. These are now well resolved, and it is clear that the exo isomer **1b** is predominant—not the endo as implied earlier. [4] The ratio was found to be approximately 60:40, and to vary little with temperature in the range 20 °C to −80 °C; the fact that the numerical ratio happens to be the inverse of that in the gas phase is presumably fortuitous. An equilibrium between endo and exo isomers of $B_4H_8 \cdot CO$ therefore exists and is influenced in solution. Similar examples are found in $B_4H_8 \cdot PF_2NMe_2$, which is exclusively endo in the crystalline state [9] and exists as both endo and exo isomers in solution (toluene-d_8 or *n*-pentane) [10], and $B_4H_8 \cdot PH_3$, which exists in one form only in the solid state and as a mixture of isomers in CD_2Cl_2 solution at −40 °C [11].

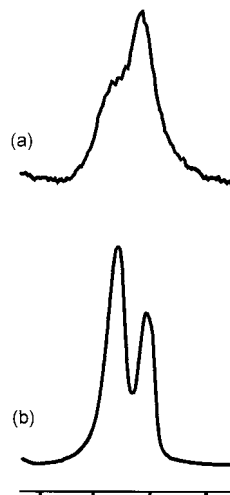It is interesting to note that the differences in chemi-

Fig. 1. (a) The region of the 128 MHz [11]B{[1]H} spectrum of $B_4H_8 \cdot CO$ in the gas phase at room temperature corresponding to boron atoms B(1), and (b) the corresponding region of the spectrum obtained on $B_4H_8 \cdot CO$ as a solution in toluene-d_8 at 238 K.

cal shifts for boron atoms B(3) (and of B(2,4)) of the endo and exo isomers are somewhat greater than those for B(1), and that the ordering of the chemical shifts is reversed; i.e. the endo isomers have less negative values than the exo isomers for B(3) and for B(2,4). In this respect, the [11]B chemical shifts for boron atoms B(3) of the endo isomers of a series of fluorophosphine derivatives, $B_4H_8 \cdot PF_2X$, were also found to be less negative than those for the exo isomers [1,11–13]. Encouragingly, all these relationships are mirrored by the computed IGLO values for $B_4H_8 \cdot CO$ [3,4].

2.2. Proton NMR data for $B_4H_8 \cdot CO$ and other B_4H_8 adducts

The single feature in the solution spectra of $B_4H_8 \cdot CO$ which most obviously distinguishes the two isomers is the chemical shift of the proton at B(1) (endo −0.18 ppm, exo 1.65 ppm). Furthermore, it was found that the endo and exo H(1) resonances provided a more accurate measure of the isomer ratio than that which could be obtained from the [11]B spectrum. To assess the possibility that the chemical shift of H(1) might be useful in identifying unknown isomers of other $B_4H_8 \cdot L$ adducts, the data for a range of such compounds have been inspected. From Table 2 it would appear that the exo isomer is dominant for L = CO, PH_3 [11], PMe_3 [12], and the sole isomer for L = $P(NMe_2)_3$ [10], NMe_3 [13] and $N_4(CH_2)_6$ [14], whereas for L = PF_2H [13] the endo form is the sole isomer in various solutions. In the case of $B_4H_8 \cdot PH_3$, there is independent evidence that

---

[3] Gas-phase ^{11}B NMR chemical shifts, δ/ppm, referenced externally to $BF_3 \cdot Et_2O = 0.0$ ppm: B_5H_{11} (8.8, 2.8 and −53.9), B_4H_{10} (−5.1 and −40.7), B_5H_9 (−12.0 and −53.9) and B_2H_6 (19.8).

[4] The wording in Ref. [1] is misleading, and appears to indicate (incorrectly) that the endo isomer was dominant in solution.

Table 1
128 MHz boron NMR data for $B_4H_8 \cdot CO$

	Calculated[a]	Gas-phase[b]	Solution[c]	
	$\delta(^{11}B)$/ppm[d]	$\delta(^{11}B)$/ppm[e]	$\delta(^{11}B)$/ppm[e]	$^1J(^{11}B-^1H_t)$/Hz[f]
endo:exo ratio	—[g]	60:40	40:60	
endo isomer, **1a**				
B(3)	3.3	4.0[h]	2.7	155[i]
B(2,4)	1.1	0.5[h]	1.1	140
B(1)	−57.6	−59.0	−59.8	137
exo isomer, **1b**				
B(3)	0.7	1.1[h]	−0.8	150[i]
B(2,4)	−1.5	0.5[h]	−1.9	133
B(1)	−57.1	−58.0	−58.7	125

[a] From IGLO calculations at II//MP2/6-31G* level (see Ref. [3]).
[b] 128 MHz, at 298 K.
[c] 128 MHz, in toluene-d_8 at 238 K, 2D $^{11}B-^{11}B\{^1H\}$ COSY showed cross peaks at (2.7 ppm, −59.8) and at (−0.8, −58.7).
[d] Referenced to $B_2H_6 = 16.6$ ppm.
[e] Referenced externally to $BF_3 \cdot Et_2O = 0.0$ ppm.
[f] ±10 Hz, from line-narrowed spectra.
[g] The endo isomer is calculated to be the more stable isomer in the gas phase by 2.5 kJ mol^{-1}.
[h] Estimated—obscured by peak overlap.
[i] $^1J_{B(3)H\mu} \sim 50$ Hz, $^1J_{B(3)B(1)} \sim 24$ Hz.

Table 2
Proton NMR data for $B_4H_8 \cdot L$

L	$\delta(^1H)$/ppm[a]			
	B(3)H	B(2,4)H[b]	B(1)H	Hμ
exo form				
CO[c], **1b**	2.79	3.05, 2.87	1.65	−2.12
PH_3[d]	2.69	2.33, 2.20	1.47	−2.02
PMe_3[e]	2.49	2.08	1.10	−2.42
$P(NMe_2)_3$[f]	2.1	2.10	0.92	−2.77
NMe_3[g]	3.11	1.99, 1.76	1.06(?)[l]	−2.04
$N_4(CH_2)_6$[h]	2.99	2.20	1.88(?)[l]	−2.08
endo form				
CO[i], **1a**	3.33	3.23, 3.00	−0.18	−2.00
PF_2H[j]	3.4	2.6	−0.1	−2.7
PF_3[k]	3.45	2.59	−0.38	−2.22

[a] Values from $^1H\{^{11}B\}$ spectra, $Me_4Si = 0.00$ ppm.
[b] Individual assignments to endo and exo protons at B(2) and B(4) not yet known.
[c] This work. 400 MHz, major isomer in toluene-d_8. Assignments determined by $^1H\{^{11}B$ selective$\}-^1H$ subtraction spectra. 2D $^1H-^1H\{^{11}B\}$ COSY spectrum showed strong cross-peaks at (2.87, 2.79), (2.87, 1.67), (2.87, −2.12) and (2.79, −2.12).
[d] Major isomer in CD_2Cl_2 at 233 K (see Refs. [4,11]).
[e] Major isomer in CD_2Cl_2 at 298 K (see Ref. [12]).
[f] Only isomer in CD_2Cl_2 at 298 K (see Ref. [10]).
[g] Only isomer in CD_2Cl_2 at 233 K (see Ref. [13]).
[h] Only isomer in CD_2Cl_2–$CDCl_3$ at 273 K (see Ref. [16]).
[i] This work. Minor isomer in toluene-d_8 at 238 K. Assignments determined by $^1H\{^{11}B$ selective$\}-^1H$ subtraction spectra. 2D $^1H-^1H\{^{11}B\}$ COSY spectrum showed strong cross-peaks at (3.33, 3.00), (3.23, −0.18) and (3.00, −2.00).
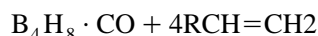[j] Only isomer; solvent and temperature unknown (see Ref. [13]).
[k] Predominant isomer; ab initio calculations predict a ratio of conformers of 98:2 endo:exo, at 296 K, and the ^{11}B NMR spectrum was consistent with this (see Ref. [15]).
[l] See Ref. [13]; there seems to be some uncertainty associated with these values.

the exo isomer is indeed dominant in CD_2Cl_2 solution, namely that the IGLO-calculated shifts [4] for the endo isomer fit best to the values reported by Jock and Kodama [11] for the minor isomer (IGLO values were not reported for the exo isomer). For the trifluorophosphine adduct, $B_4H_8 \cdot PF_3$, the endo isomer is known to comprise ca. 98% of the mixture in both the gas-phase and in $CDCl_3$ solution [15]. The endo and exo protons at B(1) in the structurally similar $B_4H_9^-$ anion [16] also differ substantially in their chemical shifts, the two values being 0.67 and −1.71 ppm. Comparison of these values with the data for $B_4H_8 \cdot CO$ suggests that the former can be assigned to the endo proton (i.e. it corresponds to the endo proton in the exo-CO form of $B_4H_8 \cdot CO$) and the latter to the exo proton.

2.3. Low-volatile products from the reactions of $B_4H_8 \cdot CO$ with ethene and propene

The reaction of $B_4H_8 \cdot CO$ with excess ethene at ca. 30 bar for 2 h at room temperature gave $Et_4B_4H_4 \cdot CO$, **2**, in 40–60% yield and with propene under similar conditions produced $Pr^n_4B_4H_4 \cdot CO$, **3**, in 50% yield.

$$B_4H_8 \cdot CO + 4RCH=CH2$$
$$\rightarrow (RCH_2CH_2)_4B_4H_4 \cdot CO \ (\mathbf{2}, R = H; \mathbf{3}, R = Me)$$

2.3.1. NMR spectra
The $^{11}B\{^1H\}$ spectrum of the low-volatile product **2** at room temperature consisted of three peaks of relative intensity 2:1:1 assigned to B(2,4), B(3) and B(1) respectively, as shown in Fig. 2(a). In the line-narrowed
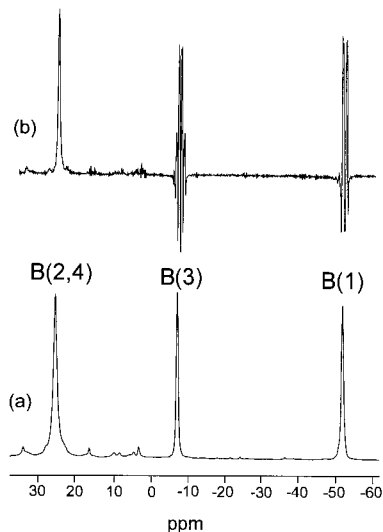
Fig. 2. (a) The 128 MHz $^{11}B\{^1H\}$ and (b) computer line-narrowed ^{11}B NMR spectra, in CD_2Cl_2 at 298 K, of the low-volatile product **2** from the reaction of $B_4H_8 \cdot CO$ and ethene.

spectrum (not shown) the signals from B(1) and B(3) were observed as doublets interpreted as partially collapsed quartets arising from $^{11}B-^{11}B$ couplings between B(1) and B(3). The ^{11}B spectrum, in the absence of proton decoupling, showed a broad singlet from B(2,4), a quartet from B(3) and a doublet from B(1). The corresponding line-narrowed ^{11}B spectrum is shown in Fig. 2(b) where the 'partially collapsed quartet' splitting is again apparent in the B(1) and B(3) resonances. The quartet pattern from B(3) indicates that the two bridge protons and the terminal proton associated with this boron atom are involved in a fluxional process at this temperature. There was no indication that either of these derivatives **2** and **3** exist as geometrical isomers in solution.

The $^1H\{^{11}B(\text{broad band})\}$ NMR spectrum of **2** at 273 K appeared as a complex multiplet at ca. 1.0 ppm, attributed to overlapping signals from the hydrocarbon and borane moieties and a broad singlet at slightly lower frequency (ca. +0.5 ppm). For boron compounds such as **2**, $^1H\{^{11}B(bb)\} - {}^1H$ subtracted spectra are useful in that they indicate which peaks arise from protons bonded to boron atoms. Subtracted spectra of this type for **2** are shown in Fig. 3, and reveal changes in the fluxionality of the protons at B(3) with change in temperature. The signal at ca. 0.5 ppm in the spectrum at 273 K, which is attributed to the three fluxional protons, is replaced in the spectrum at 223 K by a peak of intensity 2 at ca. −0.5 ppm from bridging protons, and a peak of intensity 1 at +2.2 ppm from a terminal proton. Further sharpening of the signals is observed as the temperature is lowered to 193 K. ^{13}C NMR spectra of **2** showed conclusively that two distinct ethyl groups,

i.e. exo and endo, were present. The data for **2** are listed in Table 3, together with values for **3**, the spectra for the latter being essentially analogous to those described for **2**.

In the $^1H\{^{11}B(bb)\}$ NMR spectrum of $B_4H_8 \cdot CO$ the signal from H(1) was particularly useful in defining the relative proportions of the two isomers. The presence of only one signal from H(1) in the spectra of the derivatives **2** and **3** (at 0.92 ppm and 0.6 ppm respectively) suggests that only one isomer is present in each case, as discussed earlier. If this is so, it would seem likely, from a comparison of the shift values with the data in Table 2, that the exo isomer, **2b**, is favoured for the ethene derivative. However, this conclusion is somewhat tenuous because the precise effects of the alkyl substituents on the chemical shift values are not known. An alternative possibility is that a fluxional process, such as inversion of the 'butterfly' shape about the B(1)–B(3) 'hinge', may be occurring to average the two signals. This may also apply to the adducts $B_4H_8 \cdot L$ (L = $P(NMe_2)_3$, NMe_3, $N_4(CH_2)_6$, PF_2H) where only one isomer is observed. The presence of the bulky organic groups in place of hydrogen on the wingtips is likely to lead to a widening of the butterfly angle, and a lowering of the barrier to such a process. It is possible that the fluxionality of the three protons at B(3) in **2** and **3** is also related to this process. We intend to carry out ab initio calculations on this and related systems to study this possibility. The structures of **2a** and **2b** are low-level optimisations carried out simply to generate
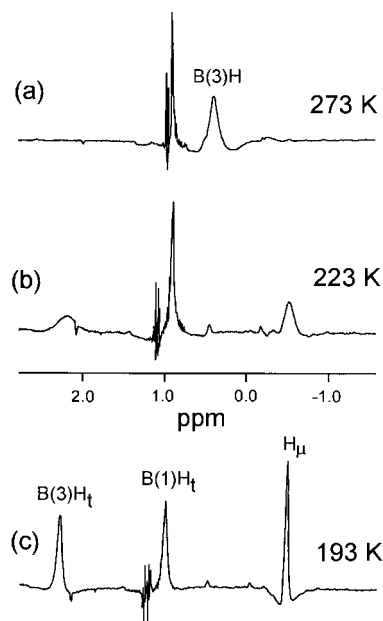

Fig. 3. $^1H\{^{11}B(bb)\} - {}^1H$ subtracted NMR spectra as a function of temperature, revealing the fluxional behaviour in $Et_4B_4H_4 \cdot CO$ **2**.

Table 3
128 MHz ^{11}B, 100 MHz ^{13}C and 400 MHz ^{1}H NMR data for $R_4B_4H_4 \cdot CO$ (R = Et, **2** or Pr^n **3**) in CD_2Cl_2 solution

Assignment	$\delta(^{11}B)$/ppm^a $\delta(^{13}C)$/ppm^b at 297 K	$^1J(^{11}B–^{11}B)$/Hz^c at 297 K	$^1J(^{11}B–^1H_t)$/Hz^c at 297 K	$\delta(^1H)$/ppm^d at 193 K
2 (R = Et)				
B(1)	−51.5	27	127	0.92
B(2,4)	26.1	—	—	—
B(3)	−6.8	28	88	2.2
H$_\mu$				−0.5
CH$_2$ ^{e}	14.4, 13.2	—	—	—^{f}
CH$_3$ ^{e}	12.7, 11.7	—	—	—^{f}
CO	180.0	—	—	—^{f}
3 (R = Pr^n)				
B(1)	−51.2	—	122	0.6
B(2,4)	24.5	—	—	—
B(3)	−6.5	—	88	3.3
H$_\mu$				−0.14
α-CH$_2$ ^{e}	26.5, 25.8	—	—	—
β-CH$_2$ ^{e}	23.0, 22.1	—	—	—
CH$_3$ ^{e}	17.8, 17.7	—	—	—
CO	179.0	—	—	—

^{a} ±0.5 ppm; referenced externally to $BF_3 \cdot Et_2O$ = 0.0 ppm, assignments supported by 2D ^{11}B–^{11}B COSY experiments.
^{b} Assignments by DEPT spectra.
^{c} ±5 Hz; from line-narrowed spectra; doublets attributed to partially collapsed quartets.
^{d} ±0.05 ppm; values from ^{1}H{^{11}B} spectra; assignments by ^{1}H{^{11}B selective} spectra.
^{e} Assignments of exo and endo groups not known.
^{f} ^{1}H data for ethyl groups of **2** in toluene-d_8 193 K, 1.18 (t, 6H, $^3J_{HH} \sim$ 7.5 Hz; CH$_3$), 1.12 (t, 6H, $^3J_{HH} \sim$ 7.5 Hz; CH$_3$), 0.96 (m†, 8H; CH$_2$); 223 K, 1.12 (t, 6H, $^3J_{HH} \sim$ 7.5 Hz; CH$_3$), 1.08 (t, 6H, $^3J_{HH} \sim$ 7.5 Hz; CH$_3$), 0.95 (m†, 8H; CH$_2$); 273 K; 1.04 (t, 6H, $^3J_{HH} \sim$ 7.5 Hz; CH$_3$), 1.02 (t, 6H, $^3J_{HH} \sim$ 7.5 Hz; CH$_3$), 0.95 (m†, 8H; CH$_2$); † denotes unresolved complex multiplet from non-equivalent protons in CH$_2$ groups in exo and endo configurations.

schematic diagrams, and no significance should be attached to the details of the structure.

2a   **2b**
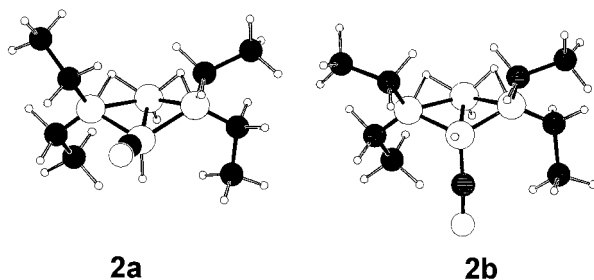
2.3.2. Infrared spectra

The CO stretch at 2155 cm^{-1} present in the gas-phase IR spectrum of $B_4H_8 \cdot CO$ remained the most obvious feature in the spectra (taken on the neat liquids) of the derivatives **2** and **3**, though there were minor shifts to lower frequency. The reduction in the intensity of the B–H stretches and the absence of any BH$_2$ scissors deformation, which appears at 1170 cm^{-1} for the parent, confirm that the hydrogen atoms on the equivalent B(2) and B(4) atoms have been substituted. The presence of the organo moieties is indicated by the C–H stretches at the 2950–2830 cm^{-1} region, and the lack of any C=C stretches indicates that these are alkyl and not alkene groups.

3. Experimental section

3.1. General

The boranes were handled in conventional high-vacuum systems equipped with greaseless O-ring taps and spherical joints (J. Young (Scientific Glassware) Ltd.). Tetraborane(8) carbonyl, $B_4H_8 \cdot CO$, was prepared from tetraborane(10), B_4H_{10}, and excess CO using a known method [5]. Tetraborane(10) was prepared by the hydride-ion abstraction reaction involving BF_3 and $Me_4NB_3H_8$ [17]; these reagents were obtained from Alfa and Aldrich respectively and used as received.

Boron and proton NMR spectra were recorded on the Bruker AM400 instrument at 9.4 T (128 MHz for ^{11}B, 100 MHz ^{13}C, and 400 MHz ^{1}H). ^{1}H{^{11}B selective} subtraction spectra [18], 2D [^{11}B–^{11}B]{^{1}H}-COSY and ^{1}H–^{1}H{^{11}B} COSY spectra [13] and DEPT spectra [19] were obtained as described in the literature. For gas-phase boron spectra, $B_4H_8 \cdot CO$ (vapour pressure ca. 71 mmHg) was admitted to a resealable NMR tube

(10 mm diameter, J. Young (Scientific Glassware) Ltd.) from a phial held at 0 °C. IR spectra were recorded on a Pye Unicam SP200 spectrometer.

3.2. Reactions of $B_4H_8 \cdot CO$ with ethene and propene

In a typical reaction, $B_4H_8 \cdot CO$ (ca. 1.0 mmol) was allowed to react for 2 h at room temperature with ethene (ca. 400 lbf in^{-2}, 30 bar) in a 75 cm^3 Hoke® single-ended stainless-steel cylinder, fitted with a Whitey® forged body shut-off valve. The cylinder was then attached to the vacuum line and cooled to the temperature of liquid nitrogen. It was then opened to a manometer and warmed slowly (30–40 min) to −131 °C (n-pentane slush bath), during which time the solvent was transferred under vacuum into a collecting trap. The cylinder was then warmed to 0 °C whilst the highly volatile components were transferred under dynamic vacuum over a period of 1 h to a U-trap immersed in liquid nitrogen. In this way the BEt$_3$ produced in the reaction was separated from the desired product. The cylinder was finally warmed to room temperature, and the product, **2**, a clear air-sensitive liquid with a vapour pressure of ca. 0.5 mmHg at 25 °C was transferred to a clean U-trap at 77 K. The yield was typically 40–60%. This method differed from that of Spielman and Burg [5] in that CO was not used to stabilise the $B_4H_8 \cdot CO$, and that much higher pressures of ethene were employed than previously. The ethene was transferred directly from the storage cylinder, whereas in the reaction with propene, the latter was first metered into a large measuring vessel and then condensed into the cylinder. Typical quantities used were: $B_4H_8 \cdot CO$ ca. 10 mmol and propene ca. 46 mmol (14 bar, 75 cm^3). The product, **3**, was obtained in yields of ca. 50% as an involatile, air-sensitive liquid with a pale yellow colour which was attributed to slight decomposition. The products from both reactions were characterised on the basis of their ^{11}B, ^{13}C and ^1H NMR spectra (see Table 3) and IR spectra of the neat liquids. IR; **1**: 2570 vs, 2515m ($v(B-H)$), 2155s ($v(C=O)$), 1950brm, 1635brw, 1535brm (BHBbr modes), 1170ms (BH$_2$ scissors bend), 1060m, 900brw, 810w cm^{-1}; **2**: 2950s, 2930m, 2910m, 2870m, 2830w (alkyl $v(C\text{-}H)$) 2510brw ($v(B-H)$), 2125s ($v(C=O)$), 1575brw, 1465m, 1435w, 1395w, 1380m, 1290w, 1110w, 1045m, 920w, 855m cm^{-1}; **3**: 2945s, 2925s, (alkyl $v(C–H)$), 2460brw ($v(B–H)$),

2105s ($v(C=O)$), 1460brs, 1390brs, 1300brs, 1105brw, 1040brw cm^{-1}. The propene derivative, **3**, had more impurity contributions, attributed to decomposition products.

References

[1] E.J. Stampf, A.R. Garber, J.D. Odom, P.D. Ellis, Inorg. Chem. 14 (1975) 2446.
[2] S.J. Cranson, P.M. Davies, R. Greatrex, D.W.H. Rankin, H.E. Robertson, J. Chem. Soc. Dalton Trans. (1990) 101.
[3] M. Bühl, P.v.R. Schleyer, Struct. Chem. 4 (1993) 1.
[4] A.M. Mebel, D.G. Musaev, K. Morokuma, Chem. Phys. Lett. 214 (1993) 69.
[5] J.R. Spielman, A.B. Burg, Inorg. Chem. 2 (1963) 1139.
[6] D. Hnyk, P.T. Brain, D.W.H. Rankin, H.E. Robertson, R. Greatrex, N.N. Greenwood, M. Kirk, M. Bühl, P.v.R. Schleyer, Inorg. Chem. 33 (1994) 2572.
[7] P.T. Brain, M. Bühl, M.A. Fox, R. Greatrex, E. Leuschner, M.J. Picton, H.E. Robertson, D.W.H. Rankin, Inorg. Chem. 34 (1995) 2841.
[8] S.J. Cranson, R. Greatrex, N.N. Greenwood, M. Whitehouse, in: G. Kabalka (Ed.), Current Topics in the Chemistry of Boron, The Royal Society of Chemistry, Cambridge, 1994, pp. 392–396.
[9] M.D. LaPrade, C.E. Nordman, Inorg. Chem. 8 (1969) 1669.
[10] J.D. Odom, T.F. Moore, W.H. Dawson, A.R. Garber, E.J. Stampf, Inorg. Chem. 18 (1979) 2179.
[11] C.P. Jock, G. Kodama, Inorg. Chem. 27 (1988) 3431.
[12] M. Kameda, M. Shimoi, G. Kodama, Inorg. Chem. 23 (1984) 3705.
[13] A.R. Dodds, G. Kodama, Inorg. Chem. 18 (1979) 1465.
[14] H. Kondo, G. Kodama, Inorg. Chem. 18 (1979) 1460.
[15] P.T. Brain, D.W.H. Rankin, H.E. Robertson, M.A. Fox, R. Greatrex, A. Nikrahi, M. Bühl, Inorg. Chem. 36 (1997) 1048.
[16] R.J. Remmel, H.D. Johnson, I.S. Jaworiwsky, S.G. Shore, J. Am. Chem. Soc. 97 (1975) 5395.
[17] M.A. Toft, J.B. Leach, F.L. Himpsl, S.G. Shore, Inorg. Chem. 21 (1982) 1952.
[18] (a) X.L.R. Fontaine, J.D. Kennedy, J. Chem. Soc. Dalton Trans. (1987) 1573. (b) X.L.R. Fontaine, J.D. Kennedy, M. McGrath, T.R. Spalding, Magn. Reson. Chem. 29 (1991) 711. (c) X.L.R. Fontaine, J.D. Kennedy, J. Chem. Soc. Chem. Commun. (1986) 779.
[19] A.E. Derome, Modern NMR Techniques for Chemistry Research, Pergamon Press, Oxford, 1987.